# Microheater platform for selective detachment of DNA

Annas Javed,[1] Samir M. Iqbal,[1,2,3,4,5] and Ankur Jain[3,6,a)]
[1]*Department of Electrical Engineering, University of Texas at Arlington, Arlington, Texas 76011, USA*
[2]*Nano-Bio Lab, University of Texas at Arlington, Arlington, Texas 76019, USA*
[3]*Nanotechnology Research and Education Center, University of Texas at Arlington, Arlington, Texas 76019, USA*
[4]*Department of Bioengineering, University of Texas at Arlington, Arlington, Texas 76010, USA*
[5]*Joint Graduate Committee of Bioengineering Program, University of Texas at Arlington and University of Texas Southwestern Medical Center at Dallas, University of Texas at Arlington, Arlington, Texas 76010, USA*
[6]*Department of Mechanical and Aerospace Engineering, University of Texas at Arlington, Arlington, Texas 76019, USA*

(Received 24 May 2012; accepted 14 August 2012; published online 30 August 2012)

Despite deoxyribonucleic acid (DNA)'s well-known temperature sensitivity, not much work has been reported on leveraging temperature to manipulate the interaction of DNA with surfaces. This paper describes a microheater device that enables the application of a temperature field on a glass surface, thereby enabling the study of temperature-dependence of DNA-surface interactions. Experimental data for thermal performance of the device agree well with finite-element simulation results. Experiments demonstrate the capability of spatially selective detachment of DNA from a glass surface using the device. The integration of thermal-based capabilities described here with analysis tools such as polymerase chain reaction may help improve DNA detection and separation capabilities. © *2012 American Institute of Physics*. [http://dx.doi.org/10.1063/1.4748308]

Site-specific detection of deoxyribonucleic acid (DNA) has been the focus of significant volume of research in past few decades for analyzing hybridization, polymerase chain reaction (PCR) amplification, and drug delivery.[1–3] The analysis of complex DNA samples and acquisition of sequence and expression information requires integration of multiple biosensors with DNA microarrays.[4,5] Miniaturization, accuracy, and capability of exposing DNA to a variety of external stimuli in DNA microarrays has played a significant role in enhancing the capabilities of genetic analysis.[6]

While the temperature-sensitivity of DNA molecules is well-known, not much work has been reported on studying how temperature and heat flow may be utilized to control and manipulate the interaction of DNA with surfaces. The governing principle behind PCR[7,8] is thermal in nature, wherein DNA is systematically manipulated by sequential thermal cycles to cause replication. However, thermal signaling in PCR occurs in a spatially independent fashion within each temperature zone and the PCR process does not utilize temperature-dependence of the chemical attachment of DNA to surfaces. It is also well known that the biotin-streptavidin bond, which is commonly used to covalently attach DNA to glass surfaces[9] has a temperature-dependent chemistry.[10] This bond has been observed to break at around 70 °C.[10] By subjecting surface-bound DNA to spatial temperature gradients, it may be possible to detach DNA from only specific locations on a microarray chip. Thermal "zones" based on an externally applied temperature field may enable selective adherence and detachment of DNA in a microarray chip. For example, based on the dependence of thermal response on DNA length and composition, it may be possible to develop thermal means for separation and highly specific replication by integrating thermal-based detachment and PCR.

Microfabricated devices offer the capability of precise control of temperature field at the microscale, enabling the study of spatial thermal effects on biological microsystems such as cells and DNA. The small thermal mass of microfabricated devices results in rapid response, high sensitivity of the temperature field, and low input power requirement.[11] Microfabricated heaters have been reported for use in gas sensors,[12,13] microvalves,[14] and thermal platforms for manipulating cells.[11,15] The capability of controlling cell behavior based on an externally applied temperature field has been reported.[11,15] However, despite the well-known temperature sensitivity of DNA and its interactions with surfaces, not much work has been reported on engineering DNA-surface interactions using thermal means.

This Letter describes a microheater device capable of subjecting DNA adhered on glass to a spatial temperature gradient. Design, microfabrication, and thermal characterization of the microheater device are presented. Experiments demonstrating the site-specific detachment of DNA from glass using thermal signals are described.

A microheater device comprising a single titanium heater wire deposited on a glass slide was microfabricated in a class-100 cleanroom using photolithography and metal deposition. The microheater width and thickness was 20 $\mu$m and 0.2 $\mu$m, respectively. The high resistivity of titanium ensured a high electrical resistance of the microheater to maximize heat generation and temperature sensitivity of the microheater resistance, which was critical for its role as a temperature sensor. Simulations described later indicated that the microheater cross-section area was large enough to rule out significant electromigration at the electric current magnitudes required for reaching the desired temperature rise. This, together with

a)Author to whom correspondence should be addressed. Electronic mail: jaina@uta.edu.

 

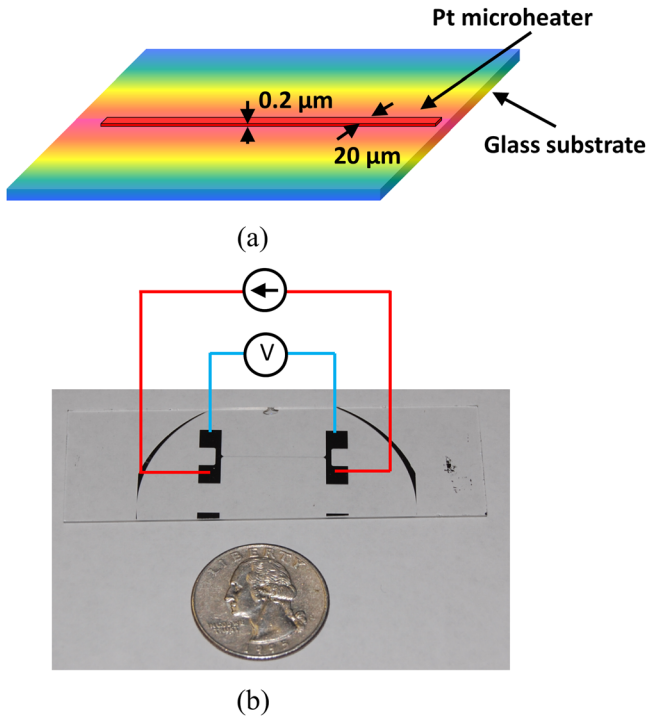


FIG. 1. (a) Schematic of the microheater device and the expected temperature field upon passing electric current. Red indicates the hottest region and blue indicates the coolest region. (b) Picture of the microheater device and the external electrical circuit utilized to drive the microheater device.

the passive nature of titanium, ensured long-term reliability of the microheater device.

Figure 1(a) shows a schematic of the microheater device and the creation of temperature zones as a result of heating in the microheater device. The region near the microheater is expected to be the hottest. Figure 1(b) shows a photomicrograph of the microheater device after fabrication and wire bonding.

Finite-element thermal simulations were carried out to determine the nature and magnitude of the transient and steady-state temperature fields in the microheater device. All simulations were carried out with around 300 K mesh elements. Transient simulations indicated that the microheater device reached thermal steady-state within around 35 s of passing electric current. Steady-state thermal simulation results for 8 mA heating current are shown in Figure 2. Figure 2(a) shows a contour plot of the temperature field around the microheater, while Figure 2(b) shows a line plot showing the temperature decay as a function of distance from the microheater. The temperature field is highest near the heater, and it decays as the distance from microheater increases. The field decays to 10% of its peak value within 6.5 mm, while the effect of the microheater is negligible beyond 12 mm. Figures 2(a) and 2(b) clearly show the formation of a space-dependent temperature field around the microheater. The magnitude and nature of this field can be varied by changing the microheater shape or the electric current, or by choosing a substrate material with different thermal conductivity.

The device was wired out in a four-wire fashion to enable simultaneous passage of current and sensing of voltage difference across the microheater. The microheater device was calibrated by measuring its electrical resistance as a function of temperature between 25 °C and 100 °C while mounted on a temperature-controlled platform in vacuum to rule out convective heat losses. A test current of only 1 $\mu$A was used for resistance measurement to minimize self-heating effects. A finite-element simulation carried out separately confirmed negligible temperature rise due to the test current. Calibration data showed that resistance was a linear function of temperature with a coefficient of $10.3 \pm 0.2\ \Omega/°C$. Based on the minimum resolution of resistance measurement on available electrical instruments, the minimum measurable temperature change was estimated to be around 0.01 °C.

Experiments were carried out to characterize the temperature rise obtained for various heating currents. Temperature rise was found to be quadratically dependent on current, as expected from the $I^2R$ nature of Joule heating. As shown in Figure 3(a), the temperature rise exhibited a linear dependence on electrical power. Experimental data were found to be in excellent agreement with results from finite-element simulation models, also plotted in Figure 3(a).

Experiments were carried out to compare the thermal performance of microheater devices fabricated on a glass slide and a coverslip. A coverslip has significantly lower

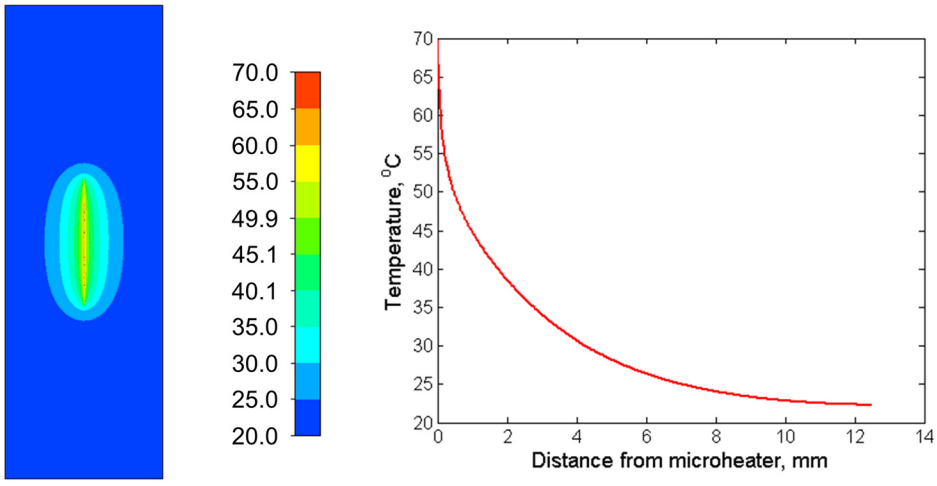


FIG. 2. (a) Contour plot of the temperature field on the microheater device determined through finite-element modeling. (b) Line plot of the temperature field showing temperature field as a function of distance from the microheater.

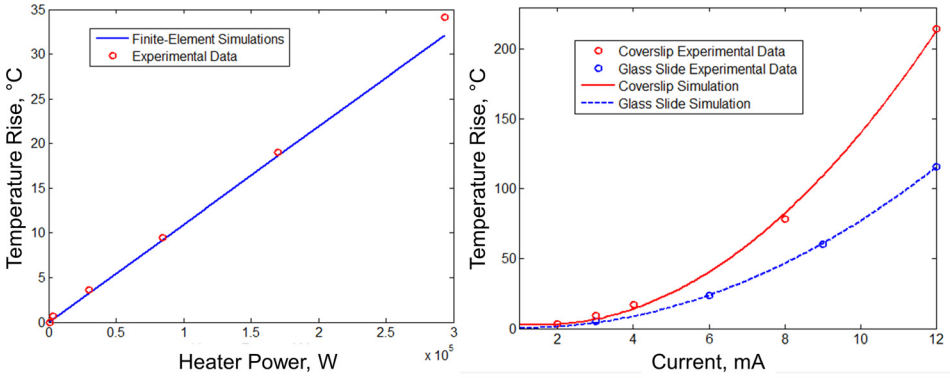


FIG. 3. (a) Comparison of measured temperature rise as a function of heating power with finite-element simulation results. (b) Comparison of the thermal performance of microheater device on a glass slide and coverslip.

thermal mass due to which the current required for reaching a given temperature rise is lower than a glass slide. In addition, the time required for reaching steady-state is also lower than a glass slide. However, microfabrication on a cover slip is challenging due to its fragile nature. Figure 3(b) compares experimental data for temperature rise as a function of heater power for a glass slide and a cover slip. A coverslip required lower current than a glass slide for reaching the same temperature rise, thereby increasing the electromigration reliability of the device. This effect was particularly pronounced at high heating powers. This showed that a cover slip may be preferable for applications where very high temperature rise is desired. However, for applications with relatively lower desired temperature, the reduction in heating current is not very significant, and may not justify additional coverslip microfabrication challenges. For example, for a temperature rise of 50 °C, the electric current requirement is 6.5 mA and 8.2 mA, respectively. All further experiments reported in this Letter were carried out on glass slides.

The attachment of DNA on inorganic surfaces such as glass is often mediated by a streptavidin-biotin based chemistry.[9,16] Typically, streptavidin is attached to glass surface through a self-assembled monolayer (SAM) of an amine-group containing a molecule such as (3-aminopropyl)triethoxysilane (APTES). Biotinlyated DNA is then covalently linked to streptavidin. It has been reported that the streptavidin-biotin bond can be broken in an aqueous solution at temperature above 70 °C.[10] Consequently, application of a spatial temperature field on DNA immobilized on glass offers a purely thermal means of spatially controlled DNA detachment. By manipulating the temperature field, it may be possible to control where on a glass chip DNA detaches and where it remains attached.

DNA was attached on a microheater fabricated on a glass slide through a streptavidin-biotin chemistry using a previously developed protocol.[9] Glass slides were first cleaned in ethanol and deionized (DI) water, and dried in nitrogen. The glass surface was amino-modified by incubation in 2 mM APTES in toluene for 1 hour at room temperature. The amino groups were coupled to biotin by incubation in 3.4 mM succinimidobiotin (NHS-biotin) in dimethyl sulfoxide (DMSO) for 1 hour at room temperature. The slides were then immersed in 1% bovine serum albumin (BSA) solution in phosphate buffered saline (PBS) for 1 hour. This step ensured that BSA occupied any uncovered portion of glass and thus prevented non-specific binding of streptavidin on glass. Finally, streptavidin was bound by incubation in 1 $\mu$M streptavidin for 30 min followed by a PBS wash. Biotinlylated DNA oligonucleotides were then applied on the surface for 30 min followed by a PBS wash. DNA sequence used in this work was 3′-biotin-AGT TCA TAT GGGC C-Texas Red-5′. Streptavidin and biotinylated DNA used in this work were fluorescently labeled with fluorescein isothiocyanate (FITC) and Texas Red, respectively. As a result, streptavidin fluoresced green when excited at around 495 nm, while DNA fluoresced red when excited at around 589 nm. Both fluorescence emissions were examined independently using a fluorescence microscope and appropriate filter cubes. Figure 4 shows the surface binding chemistry utilized for DNA attachment.

Experiments were first carried out to confirm the attachment of DNA using the protocol described above. Functionalization with only streptavidin resulted in green fluorescence using a FITC filter cube but no red fluorescence with the Texas Red filter cube. A slide functionalized with streptavidin followed by DNA showed red fluorescence in the Texas Red filter cube, but no green fluorescence in the FITC filter cube. The observed fluorescence persisted even after washing the prepared glass slides with DI water or PBS, and the wash did not exhibit any fluorescence. These experiments indicated that the protocol described above effectively attached DNA to the glass surface.

The microheater device was then heated up to 75 °C with the functional area of the microheater device immersed in DI water. The electrical current was increased until the microheater resistance corresponded to the expected value at 70 °C, as determined from prior thermal calibration. The electrical current was passed for 2 min, which according to transient finite-element simulations was sufficient time for the steady temperature field to set up. Figure 5 shows fluorescent images before and after turning the heater on. Since the microheater line itself has no fluorescence, it is not visible in

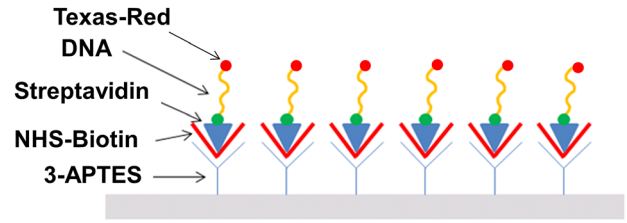


FIG. 4. Schematic diagram of the surface binding chemistry utilized for immobilizing DNA on a glass surface.

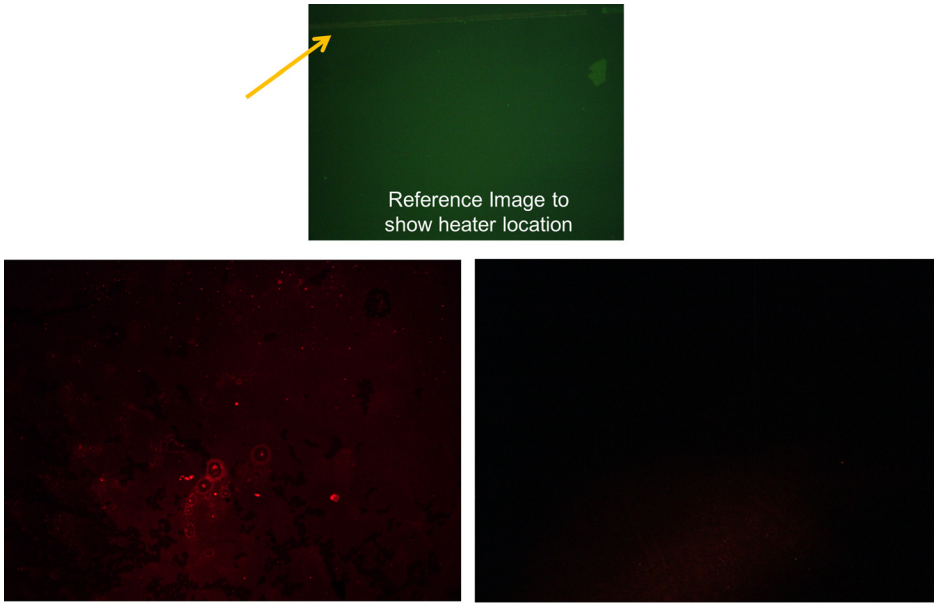


FIG. 5. Fluorescent images before and after heating the microheater device. A reference image shows the approximate location of the microheater.

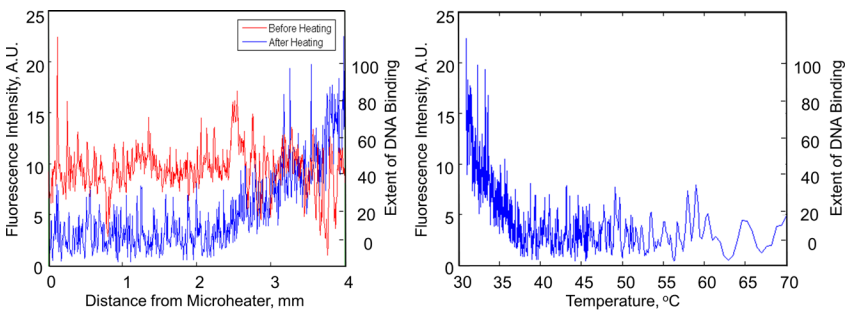


(a) (b)

FIG. 6. (a) Comparison of quantitative fluorescence intensity and extent of binding as a function of distance before and after heating. (b) Fluorescence intensity and extent of binding as a function of temperature.

the images. However, the reference image in Figure 5, obtained with incident white light, shows the microheater running from left to right on the top of the image. All images were taken at approximately the same location of the device. It was observed that as a result of heating, the red fluorescence indicative of DNA decreased substantially in regions close to the microheater, whereas the reduction in fluorescence was not significant farther away from the heater. This is confirmed by quantitative fluorescence measurement shown in Figure 6(a) as a function of distance from the microheater. Fluorescence intensity is extracted using ImageJ software. DNA fluorescence is spatially uniform prior to heating. After heating, there is substantial reduction in intensity close to the heater, and as distance increases, the intensity increases linearly back to the before-heating level. This indicates that while the microheater influenced DNA immobilization close to the heater, the effect was negligible farther away from the heater. This was consistent with the temperature field obtained from finite-element simulations, which indicated a space-limited thermal influence zone around the heater. No reduction in intensity was observed if no current was passed through the heater line, or if the current was too small to result in a significant temperature rise. This showed that the high temperature in regions close to the microheater line specifically broke the chemical bonds responsible for immobilizing streptavidin-DNA on the glass surface. The spatial temperature field obtained from finite-element simulations, shown in Figure 2(b) can be used to determine the extent of DNA attachment as a function of temperature. This is plotted in Figure 6(b), which shows that fluorescent intensity and the extent of DNA attachment reduces as temperature increases, eventually saturating around 50 °C. Note that the DNA attachment is quantified in terms of the fluorescent intensity from the Texas Red fluorophore located on the 5′ of the DNA, since only DNA attached to the surface is capable of fluorescing, whereas any unattached DNA is washed away in the wash steps carried out prior to fluorescence measurement. Moreover, fluorescence of Texas Red is a very weak function of temperature in the temperature range of interest.[17]

It is expected that this work may enable the development of DNA analysis microdevices wherein sophisticated temperature zones are defined to enable DNA to be detached only from desired locations in a glass-based DNA analysis chip. Such an exercise may utilize thermal simulations discussed previously to reverse-engineer the microheater line pattern required to produce a desired temperature map. Integration of thermal-based detachment of DNA from glass surfaces with analysis assays such as PCR may enable new capabilities of detection and separation in DNA analysis microdevices.

Microfabrication described in this work was carried out at Nanotechnology Research and Education Center at the University of Texas, Arlington.

[1]J. Khandurina, T. E. McKnight, S. C. Jacobson, L. C. Waters, R. S. Foote, and J. M. Ramsey, Anal. Chem. **72**, 2995 (2000).
[2]J. Wang, Talanta **56**, 223 (2002).
[3]B. J. Hindson, D. M. Gutierrez, K. D. Ness, A. J. Makarewicz, T. R. Metz, U. S. Setlur, W. B. Benett, J. M. Loge, B. W. Colston, P. S. Francis, N. W. Barnett, and J. M. Dzenitis, Analyst **133**, 248 (2008).
[4]A. Sassolas, B. D. Leca-Bouvier, and L. J. Blum, Chem. Rev. **108**, 109 (2008).
[5]R. Levicky and A. Horgan, Trends Biotechnol. **23**, 143 (2005).
[6]A. Schulze and J. Downward, Nat. Cell Biol. **3**, E190 (2001).
[7]K. B. Mullis and F. A. Faloona, Methods Enzymol. **155**, 335 (1987).
[8]R. K. Saiki, D. H. Gelfand, S. Stoffel, S. J. Scharf, R. Higuchi, G. T. Horn, K. B. Mullis, and H. A. Erlich Science **239**, 487 (1988).
[9]A. Kasry, P. Borri, P. R. Davies, A. Harwood, N. Thomas, S. Lofas, and T. Dale, ACS Appl. Mater. Interfaces **1**, 1793 (2009).
[10]A. Holmberg, A. Blomstergren, O. Nord, M. Lukacs, J. Lundeberg, and M. Uhlen, Electrophoresis **26**, 501 (2005).
[11]A. Jain, K. D. Ness, and K. E. Goodson, Sens. Actuators, B **143**, 286 (2009).
[12]G. Sberveglieri, W. Hellmich, and G. Müller, Microsyst. Technol. **3**, 183 (1997).
[13]D. Briand, S. Heimgartner, M.-A. Grétillat, B. van der Schoot, and N. F. de Rooij, J. Micromech. Microeng. **12**, 971 (2002).
[14]M. Kohl, D. Dittmann, E. Quandt, B. Winzek, S. Miyazaki, and D. M. Allen, Mater. Sci. Eng., A **273**, 784 (1999).
[15]W. Shu, W. N. Everett, Q. X. Zhang, M. H. Liu, A. Trigg, Y. Ma, S. M. Spearing, S. Wang, H.-J. Sue, and P. M. Moran, IEEE J. Microelectromech. Syst. **14**, 924 (2005).
[16]Q. Du, O. Larsson, H. Swerdlow, and Z. Liang, "DNA immobilization: Silanized nucleic acids and nanoprinting," in *Immobilisation of DNA on Chips II*, edited by C. Wittmann (Springer, 2006), Vol. 261, pp. 45–62.
[17]Y. You, A. Tataurov, and R. Owczarzy, Biopolymers **95**, 472 (2011).